Evaluation of Reliability of Coats-Redfern and Criado Methods for Kinetics Analysis of Olive Mill Solid Waste and Olive Mill Wastewater

M. Y. Guida, A. Hannioui

Abstract— Study of the decomposition kinetics is an important tool for the developpement of recycling and treat olive mill wastes to produce valuable products. In this work, the activation energy and the reaction model of the pyrolysis of olive mill wastes such as, olive mill solid waste (OMSW) and concentrated olive mill wastewater (COMWW) have been estimated from non-isothermal kinetic results. Firstly the activation energy values obtained by KAS method in comparison with Friedman (FR), Vyazovkin (VYA) and Flynn-Wall-Ozawa (OFW) isoconversional methods are: 150-176 KJ/mol for hemicellulose and 212-235 KJ/mol for cellulose of OMSW and 132-154 KJ/mol for hemicellulose and 237-283 KJ/mol for cellulose of COMWW. Secondly, the appropriate conversion model of the process was determined by Coats-Redfern and Criado methods. The pyrolysis reaction models of OMSW and COMWW are described by reaction order F_n, second order (F_2) for cellulose and hemicelluloses of OMSW and COMWW. Whereas the hemicelluloses of OMSW and COMWW following a kinetic model of F_1 (First order) and D_1 (One-dimensional diffusion), respectively.

Index Terms— Olive mill solid waste, Olive mill wastewater, Pyrolysis, Activation energy, Coats-Redfern method, Criado method.

1 Introduction

The olive oil industry is very important in Mediterranean countries, both in terms of wealth and tradition [1]. The extraction of olive oil generates huge quantities of wastes that may have a great impact on land and water environments because of their high phytotoxicity [2]. For many years, olive mill wastes such as olive mill solid waste (OMSW) and olive mill wastewater (OMWW) have been the most pollutant and troublesome wastes produced by olive mill in Mediterranean countries. Thus, the treatment and management of this solid and liquid residue has been extensively investigated and some extensive and detailed reviews, which focus mainly on its treatment, have been recently published [3-7].

Thermal degradation of olive mill wastes such as olive mill solid waste and concentrated olive mill wastewater have great interest as an alternative source of energy or chemical raw materials, as well as it contributes to the solution of environment problems caused by olive mill wastes. The determination of the parameters of the thermal decomposition process by means of thermogravimetric techniques allows the development of the recycling process of these materials in an industrial scale [8-10]. A thermogravimetric analysis (TGA) technique is an excellent way for studying the kinetics of thermal degradation it provides information on activation energy and kinetic model.

Many studies [11-17], on pyrolysis of olive mill wastes have been carried out, and most of these studies have been developed on the assumption that the reaction can be described by a nth order reaction model. The assumption of a nth order reaction model would result in the Arrhenius parameters deviating from the real ones. Few attempts, however, have been made to identify the reaction model of the olive mill waste pyrolysis. Isothermal reduced-time plots have been applied to determine the reaction model of the thermal decomposition of solids [18-21].

The aim of this work is specially to show the reliability of Coats-Redfern and Criado methods for kinetics analysis of olive mill solid waste and concentrated olive mill wastewater. These are new attempts for thermochemical of wastes in new applying Criado and Coats-Redfern methods to identify the pyrolysis reaction model, possibility contributing to the research field of pyrolysis kinetics of thermochemical of olive wastes.

In this work, the thermogravimetric study of olive mill solid waste (OMSW) and concentrated olive mill wastewater (COMWW) was realized using non-isothermal method in order to determine the apparent activation energy and the pyrolysis reaction model.

2 Experimental Procedure

2.1 Materials and Samples Preparation

The olive wastes samples used in this research work was obtained from the Béni-Mellal area which located about 303 Km of Rabat and was sampled from the olive oil process (Mâasra in Morocco). The olive mill wastewater samples were concentrated via evaporation with a rotating evaporator at atmosphere pressure to a concentrated remainder that could then be dried to a residue: on the other hand, the olive solid waste samples were-air-dried and both samples were ground to obtain a uniform material of an average particle size (0.1-0.2 mm). Table 1 shows the chemical compositions of samples while the physical-chemical characterization of the raw OMWW depicted in table 2.

- *Mohamed Yassine Guida, Laboratoire de chimie organique et analytique, Faculté des sciences et techniqus de Béni-Mellal, Université Sultan Moulay Slimane, Béni-Mellal, Morocco.*
- *Abdellah Hannioui Laboratoire de chimie organique et analytique, Faculté des sciences et techniqus de Béni-Mellal, Université Sultan Moulay Slimane, Béni-Mellal, Morocco.*

2.2 TGA Experiments

Olive mill solid waste (OMSW) and concentrated olive mill wastewater (COMWW) samples were subjected to TG in an inert atmosphere of nitrogen. Rheometrix Scientific STA 1500 TGA analyzer was used to measure and record the sample mass change with temperature over the course of the pyrolysis reaction. Thermogravimetric curves were obtained at four different heating rates (5, 10, 20 and 50 °C.min^{-1}) between 25 and 900 °C. Nitrogen gas was used as an inert purge gas to displace air in the pyrolysis zone, thus avoiding unwanted oxidation of the sample. A flow rate of around 60 mL.min^{-1} was fed to the system from a point below the sample and a purge time of 60 min (to be sure the air was eliminated from the system and the atmosphere is inert). The balance can hold a maximum of 45 mg; therefore, all sample amounts used in this study averaged approximately 20 mg. The reproducibility of the experiments is acceptable, and the experimental data presented in this paper corresponding to the different operating conditions are the mean values of runs carried out two or three times.

TABLE 1
MAIN CHARACTERISTIC OF OMSW AND COMWW

	OMSW /%	COMWW /%
Proximate analysis		
Moisture	8.3	3.8
Volatile matter	73.5	61.4
Ash	4.5	25.1
Fixed carbon	13.7	9.7
Elemental analysis		
C	45.5	39.7
H	5.3	4.6
N	1.8	1.7
O	47.4	46
Chemical analysis		
Hemicellulose	21.6	17.4
Cellulose	30.4	23.3
Lignin	43.5	34.2

.3 Theoretical consideration

The pyrolysis process may be represented by the following reaction scheme [22, 23]:

$$S_{\text{(solid)}} \text{--------} > C_{\text{(solid)}} + V_{\text{(volatile)}}$$

The rate of conversion, dx/dt for TG experiment at constant rate of temperature change, $\beta=dt/dT$ may be expressed by:

$$\frac{dx}{dt} = k(T).f(x) \qquad (1)$$

Where x is the degree of advance defined by:

$$x = \frac{m_0 - m_t}{m_0 - m_\infty} \qquad (2)$$

Where m_t is the weight of the sample at a given time t, m_0 and m_∞, refer to values at the beginning and the end of the weight loss event of interest. $f(x)$ and $k(T)$ are functions of conversion and temperature, respectively. $k(T)$, the temperature dependence of the rate of weight loss, is often modeled successfully by the Arrhenius equation :

$$K(T) = A.\exp(\frac{-E}{RT}) \qquad (3)$$

Where E is the activation energy, A is the pre-exponential factor and R the gas constant. By combining the Eqs. (1) and (3), the reaction rate can be written in the form:

$$\frac{dx}{dT} = \frac{A_x}{\beta}.\exp(\frac{-E}{RT}).f(x) \qquad (4)$$

$$with: \quad \beta = \frac{dT}{dt}$$

2.3.1 Kissinger-Akahira-Sunose method (KAS)

The standard Eq (4) can be written [24, 25], as follows:

$$\frac{dx}{f(x)} = \frac{A_x}{\beta}.\exp(\frac{-E}{RT_m}).f(x) \qquad (5)$$

Which is integrated with the initial condition of $x=0$ et $T=T0$ to obtain the following expression:

$$g(x) = \int_0^x \frac{dx}{f(x)} = \frac{A}{\beta}\int_{T_0}^{T} \exp(\frac{-E}{RT_m}) \cong \frac{AE}{\beta R} p(\frac{E}{RT_m}) \qquad (6)$$

Essentially the technique assumes that the A, $f(x)$ and E are idependent of T while A, $f(x)$ and E are independent of x, then Eq. (6) may be integrated to give the following equation in logarithmic form:

$$\ln g(x) = \ln(\frac{AE}{R}) - \ln \beta + \ln p(\frac{E}{RT_m}) \qquad (7)$$

TABLE 2
PHYSICAL CHEMICAL DETERMINATION OF THE RAW OMWW

Parameters	Valeurs
pH (25 °C)	5.15
Electrical conductivity Ms/cm à 20 °C	6.73
Total phenols g/L	13.35
Total COD gO_2/l	70.40

The KAS method is based on the Coats-Redfern approximation according to which:

$$p(\frac{E}{RT_m}) \cong \frac{\exp(\frac{-E}{RT_m})}{(\frac{E}{RT_m})} \qquad (8)$$

TABLE 3
ALGEBRAIC EXPRESSIONS OF FUNCTIONS OF THE MOST COMMON REACTION MECHANISMS

	Mechanism	*f(x)*	*g(x)*
Diffusion D_n	One dimensional diffusion-**D1**	$1/2x^{-1}$	x^2
	Two dimensional diffusion-**D2**	$[-\ln(1-x)]^{-1}$	$[(1-x)\ln(1-x)]+x$
	Three dimentional diffusion, Jander-**D3**	$3/2(1-x)^{2/3}[1-(1-x)^{1/3}]^{-1}$	$[1-(1-x)^{1/3}]^2$
	Ginstling-Brounshtein-**D4**	$3/2[(1-x)^{-1/3}-1]$	$1-(2x/3)-(1-x)^{2/3}$
Reaction order F_n	First-order 1-**F1**	$(1-x)$	$-\ln(1-x)$
	Second-order 2-**F2**	$(1-x)^2$	$(1-x)^{-1}-1$
	Third-order 3-**F3**	$(1-x)^3$	$[(1-x)^{-2}-1]/2$
Power law P_n	Power law-**P2**	$2x^{1/2}$	$x^{1/2}$
	Power law-**P3**	$3x^{2/3}$	$x^{1/3}$
	Power law-**P4**	$4x^{3/4}$	$x^{1/4}$
Avrami-Erofe've A_n	Avrami-Erofe've-**A2**	$2(1-x)[-\ln(1-x)]^{1/2}$	$[-\ln(1-x)]^{1/2}$
	Avrami-Erofe've-**A3**	$3(1-x)[-\ln(1-x)]^{2/3}$	$[-\ln(1-x)]^{1/3}$
	Avrami-Erofe've-**A4**	$4(1-x)[-\ln(1-x)]^{3/4}$	$[-\ln(1-x)]^{1/4}$
Contraction reaction R_n	Contraction sphere-**R2**	$2(1-x)^{1/2}$	$[1-(1-x)^{1/2}]$
	Contraction cylinder-**R3**	$3(1-x)^{2/3}$	$[1-(1-x)^{1/3}]$

From relationships (6) and (8) it follows that:

$$\ln\frac{\beta}{T_m^2} = \ln(\frac{AR}{E.g(x)}) - \frac{E}{RT} \qquad (9)$$

2.3.2 Coats-Redfern method

Coats-Redfern method [26, 27] is also an integral method, and it involves the thermal degradation mechanism. Using an asymptomatic approximation for resolution of Eq.(6) (*2RT/E<<1*) the following equation can be obtained:

$$\ln\frac{g(x)}{T^2} = \ln(\frac{AR}{\beta.E}) - \frac{E}{RT} \qquad (10)$$

2.3.3 Criado method

If the value of the activation energy is known, the kinetic model of the process can be determined by this method [28]. Combining the Eq.(5) with Eq.(10), the following equation is obtained:

$$\frac{Z(x)}{Z(0.5)} = \frac{f(x).g(x)}{f(0.5).g(0.5)} = \left(\frac{T_x}{T_{0.5}}\right)^2 \frac{(dx/dt)_x}{(dx/dt)_{0.5}} \qquad (11)$$

Where 0.5 refers to the conversion in *x=0.5*
The left side of Eq.(11) *f(x).g(x)/f(0.5).g(0.5)* is a reduced theoretical curve, which is characteristic of each reaction mechanim, whereas the right side of the equation associated with the reduced rate can be obtained from experimental data. A comparison of both sides of Eq.(11) tells us which kinetic model describes an experimental reactive process. Table 3 indicates the algebraic expressions of *f(x)* and *g(x)* for kinetic models used.

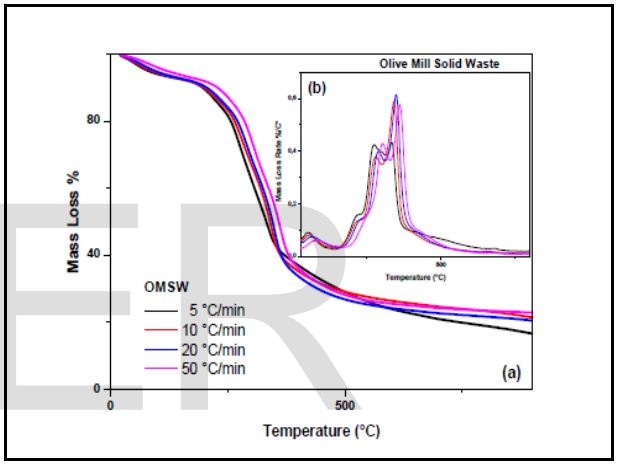

Fig. 1. TG and DTG of OMSW, (a) TG, (b) DTG

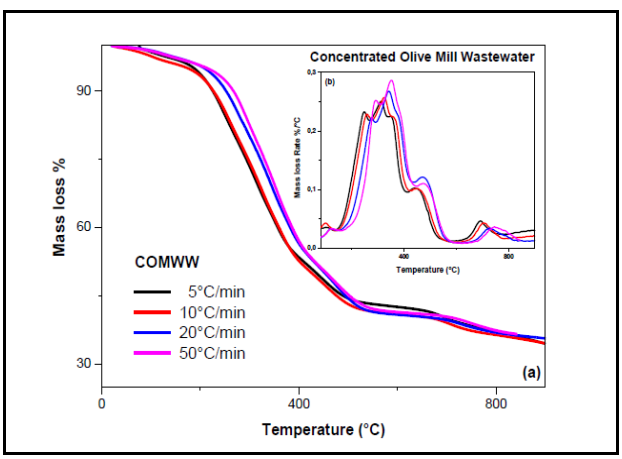

Fig. 2. TG and DTG of COMWW, (a) TG, (b) DTG

3 Results and Discussion

3.1 Thermal degradation

Figs 1 and 2 show the TG/DTG curves for olive mill wastes such as olive mill solid waste and concentrated olive mill wastewater at different heating rates (5, 10, 20 and 50 °C/min). Different temperature values of OMSW and COMWW are summarized in tables 4 and 5. The weight losses (TG) show that degradation of OMSW and COMWW occur almost in three different temperature regimes: drying, main devolatilization and continuous slight develatilization. During drying stage, the mass loss is approximately 3.4% for COMWW and 8% for OMSW. Thermal decomposition reaction took place in the temperature range of about 150-434 °C producing non-condensable and condensable volatile gases. The main devolatilization of the OMSW and COMWW starts at 163 and 150 °C respectively. The devolatilization step finishes later (450 °C) for OMSW compared to COMWW (434 °C).

This behavior may be related to the original composition of OMSW being richer in cellulose relative to COMWW. The weight losses of the main pyrolysis are 46.2 % and 57.8 % for COMWW and OMSW, respectively. This phenomenon is in full accordance with the highest percentages of ash in COMWW and lowest percentage of ash in OMSW approximate analysis. Comparing TG (Thermogravimetric) and DTG, one can say that the two samples differ in reactivity. The COMWW and OMSW samples revealed large differences in their decomposition behavior.

TABLE 4
DIFFERENT TEMPERATURE VALUES OF OMSW

sample	Heating rate / °C.min^{-1}	First step /°C $T_i/T_{max1}/T_f$	Second step /°C $T_i/T_{max2}/T_f$
OMSW	5	162/273/296	296/333/381
	10	171/279/302	302/338/394
	20	184/291/311	311/350/413
	50	204/302/329	329/363/404

TABLE 5
DIFFERENT TEMPERATURE VALUES OF COMWW

sample	Heating rate / °C.min^{-1}	First step /°C $T_i/T_{max1}/T_f$	Second step /°C $T_i/T_{max2}/T_f$
COMWW	*5*	*150/239/262*	*262/304/403*
	10	*161/257/274*	*274/320/416*
	20	*167/261/277*	*277/324/423*
	50	*175/273/294*	*294/336/434*

The initial temperature of degradation is higher in OMSW, which present high amount of cellulose in comparison with COMWW and that is in fluke with literature. The difference in the fraction of cellulose and hemicelluloses between two materials is relatively greater, which indicates that the different properties of the pyrolysis process between OMSW and COMWW are mainly affected by the percentage of cellulose and hemicelluloses. After main pyrolytic process, there is slow and continuous degradation between 400 and 600 °C attributed to lignin degradation. In the case of COMWW, a slight mass loss between 600 and 800 °C can be assigned to the decomposition of inorganic material.

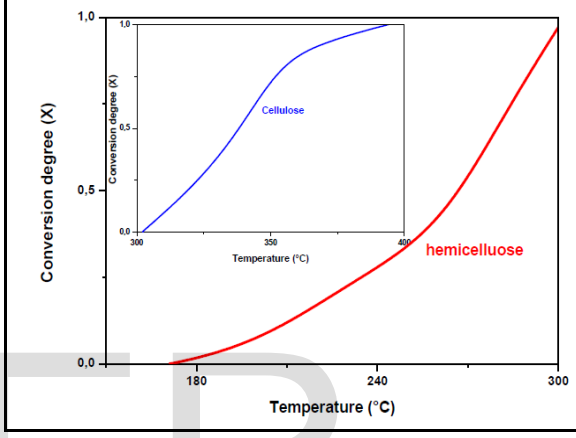

Fig. 3. Variation of conversion (x) as function of temperature at 10 °C/min for hemicelluloses and cellulose of OMSW

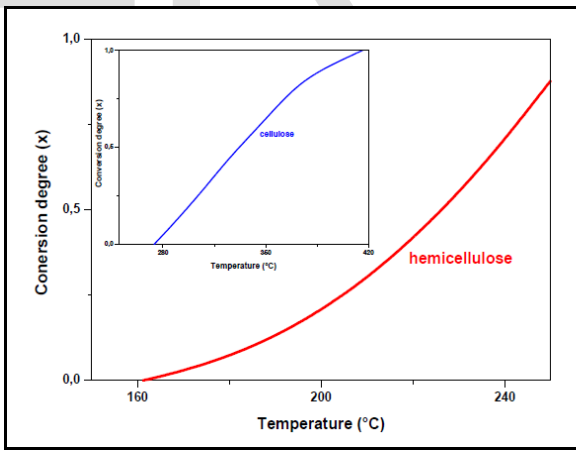

Fig. 4. Variation of conversion (x) as function of temperature at 10 °C/min for hemicelluloses and cellulose of COMWW

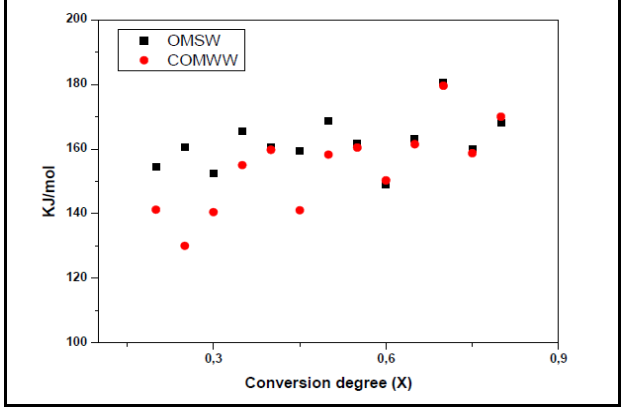

Fig. 5. Dependence of activation energy on conversion degree (x) according to KAS method for decomposition of hemicelluloses for OMSW and COMWW

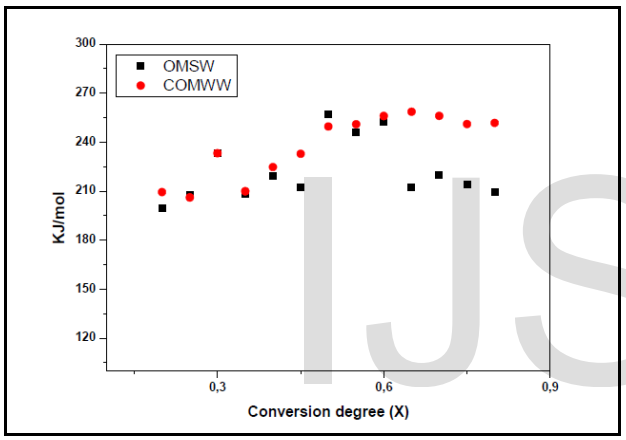

Fig. 6. Dependence of activation energy on conversion degree (x) according to KAS method for decomposition of cellulose for OMSW and COMWW

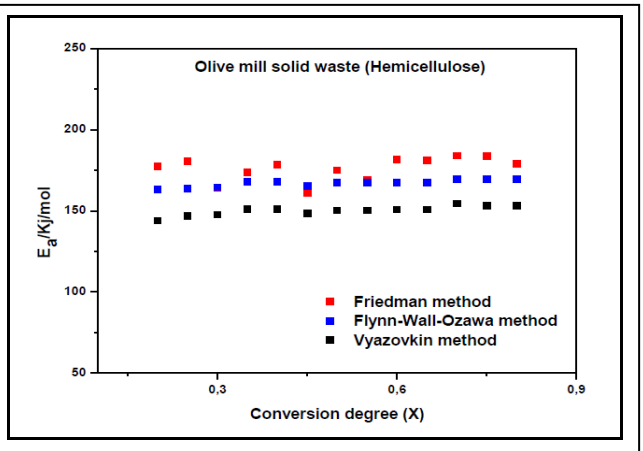

Fig. 7. Dependence of activation energy on conversion degree (x) according to VYA, OFW and FR methods for decomposition of hemicellulose for OMSW

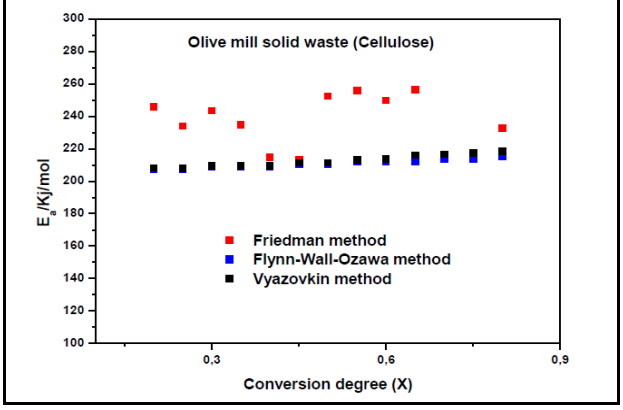

Fig. 8. Dependence of activation energy on conversion degree (x) according to VYA, OFW and FR methods for decomposition of cellulose for OMSW

The decomposition rate of OMSW is higher than COMWW (DTG_{max} value). The values obtained for this parameter confirms the lower reactivity of COMWW in comparison with OMSW. Residual masses at 850 °C are 35.6 % for the initial mass for COMWW and 21.5 % for OMSW. This behavior may be due to the presence of polyaromatic compounds which need higher temperature to be thermally destroyed. Furthermore, with regard to the literature and our study, COMWW has high inorganic salt content which may explain the high amount of ash in the COMWW sample.

One of the most important parameters influencing the pyrolysis characteristics is heating rate. From figs 1, 2 and tables 4, 5. One can say that the heating rate affects significantly the maximum decomposition rate, with maximum decomposition rate tending to increase and occur at higher temperatures when pyrolyzed at higher heating rates and this can be interpreted by the fact that biomass (OMSW and COMWW) has a heterogeneous structure and possesses a number of constituents. These constituents gave their characteristic individual decomposition peaks in definite temperature ranges in the pyrolysis process. When heating rate was sufficiently low during pyrolysis, most of these peaks can be seen as small broken lines or vibrations. At high heating rates, separate peaks did not arise because some of them were decomposed simultaneously and several adjacent peaks were united to form overlapped boarder and higher peaks. This fact can be a consequence of heat and mass transfer limitations. With an increase in heating rate, the temperature in the furnace space can be a little higher as the temperature of a particle and the rate of decomposition are higher than the release of volatiles.

3.2 The kinetics of thermal decomposition

For the calculation of the activation energies, all four heating rates have been used and they were estimated using the Kissinger-Akahira-Sunose (KAS) method compared with Friedman (FR), Vyazovkin (VYA) and Flynn-Wall-Ozawa (OFW) methods which are already used in our work [29, 30].

$$\ln(\frac{dx}{dt}) = \ln(f(x).A_x) - \frac{E}{RT_x} \qquad (12)$$

$$\ln(\beta) = \ln\left(\frac{AE}{Rg(x)}\right) - 5.331 - 1.052\frac{E}{RT_x} \qquad (13)$$

$$\ln(\frac{\beta}{T^2}) = \ln\left(\frac{RA_x}{Eg(x)}\right) - \frac{E}{RT_x} \qquad (14)$$

Firstly, the isoconversional Kissinger-Akahira-Sunose method Eq. (9), was used to calculate the activation energy for different conversion values by plotting *ln (β/T²)* against *1/T*, in correlation coefficient *(R^2)* higher than 0.995 and the results are shown in Figs 5,6 and table 6. For OMSW and COMWW (with both compounds: cellulose and hemicelluloses). The mean values of activation energy were 161.84 and 222.35 Kj/mol for hemicelluloses and cellulose of OMSW, and were 154.29 and 237.70 Kj/mol for hemicelluloses and cellulose of COMWW. Secondly, the isoconversional Friedman, Vyazovkin methods and the integral Ozawa-Flynn-Wall method were used in our work within the framework of study of olive mill wastes. The Friedman method Eq. (12) was used to calculate the activation energy for different conversion values by plotting of *ln (dx/dT)* against *1/T* for a constant value and calculated the activation energy, figs 11 and 14. The mean values of activation energy were 176 Kj/mol, 235 Kj/mol for hemicelluloses and cellulose of OMSW, and 146 Kj/mol, 283 Kj/mol for hemicelluloses and cellulose of COMWW. The Vyazovkin method Eq. (14), was used to calculate the activation energy for different conversion values by plotting *ln (β/T²)* against *1/T* (figs 13 and 16) and the mean values of activation energy were 150 Kj/mol, 212 Kj/mol for hemicelluloses and cellulose for OMSW, and 132 Kj/mol, 255 Kj/mol for hemicelluloses and cellulose of COMWW. Flynn-Wall-Ozawa method Eq. (13) (figs 12 and 15), is an integral method which is also independent of the degradation mechanism, it has been used and the activation energy of OMSW and COMWW was obtained from plot of *ln (β)* against *1/T* at a fixed conversion with the slope of such a line being 0.4567E/RT. The mean values of activation energy were 167 Kj/mol, 215 Kj/mol for hemicelluloses and cellulose of OMSW, and 137 Kj/mol, 255 Kj/mol for hemicelluloses and cellulose of COMWW.

TABLE 6
ACTIVATION ENERGY (E_A) DEDUCED FROM KAS METHOD OF OMSW AND COMWW

Conversion degree	OMSW (Kj/mol)		COMWW (Kj/mol)	
x	Hemicellulose	Cellulose	Hemicellulose	Cellulose
0.2	154,38	199,59	141,2	209,45
0.25	160,52	207,49	130	206
0.3	152,51	232,94	140,44	233,2
0.35	165,41	208,14	155,01	210
0.4	160,43	219,03	159,68	224,74
0.45	159,28	212,51	141,02	232,85
0.5	168,69	257,01	158,24	249,59
0.55	161,73	246	160,36	250,9
0.6	149,08	252,46	150,31	256,08
0.65	163,2	212,28	161,42	258,63
0.7	180,67	220,02	179,54	256
0.75	160,01	213,86	158,64	251
0.8	168,12	209,34	170	251,69
Mean	161,84	222,35	154,29	237,70

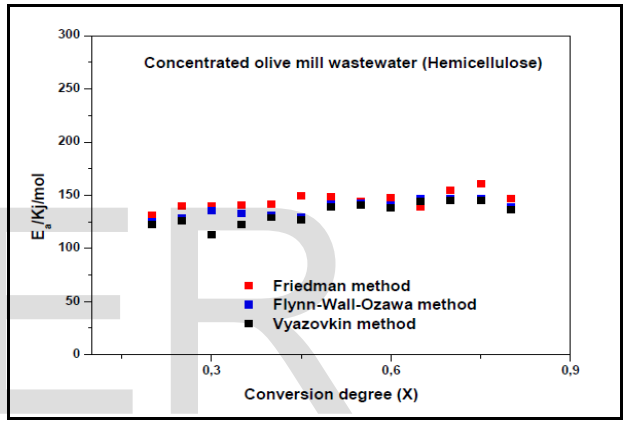

Fig. 9. Dependence of activation energy on conversion degree (x) according to VYA, OFW and FR methods for decomposition of hemicellulose for COMWW

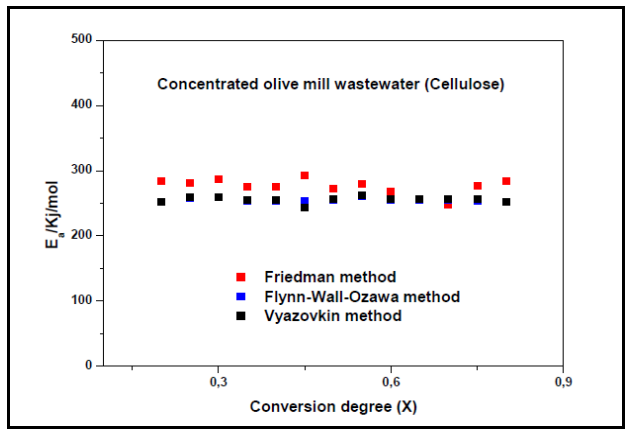

Fig. 10. Dependence of activation energy on conversion degree (x) according to VYA, OFW and FR methods for decomposition of cellulose for COMWW

Figs 7-10, shows the dependence of activation energy on the conversion degree for x=0.2-0.8 for hemicelluloses and hemicelluloses of OMSW and COMWW, with an increment of 5 % (x=0.05). The FWO and VYA give similar values of E in x range while the values achieved by the Friedman method were larger than those obtained by FOW and VYA. The differences in calculated E values can also be caused due to the error of improper integration in FWO and VYA equations. Friedman method was instantaneous values and so very sensitive to the experimental noises. Concerning the Kissinger method (KAS), one can say that it has the same tendency, small variations are observed. The difference in determined values of activation energy by KAS and other methods can be expected, for example; the FWO and KAS methods involve a systematic error in activation energy that does not appear in the Friedman method.

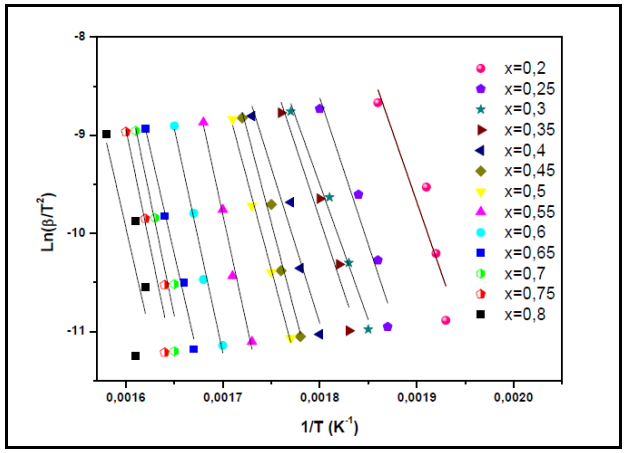

Fig. 13. Vyazovkin plots for hemicellulose of OMSW thermal degradation

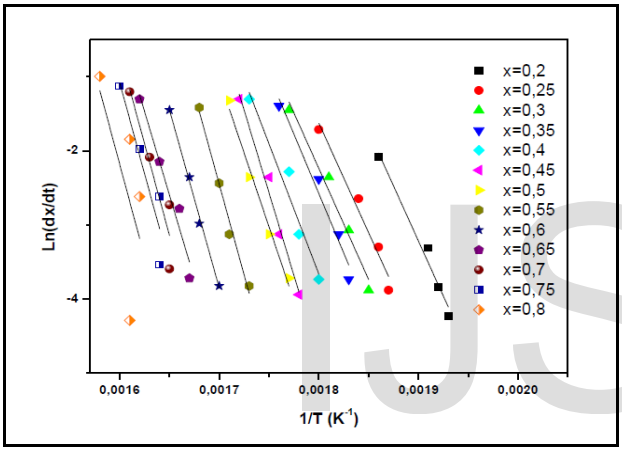

Fig. 11. Friedman plots for hemicellulose of OMSW thermal degradation

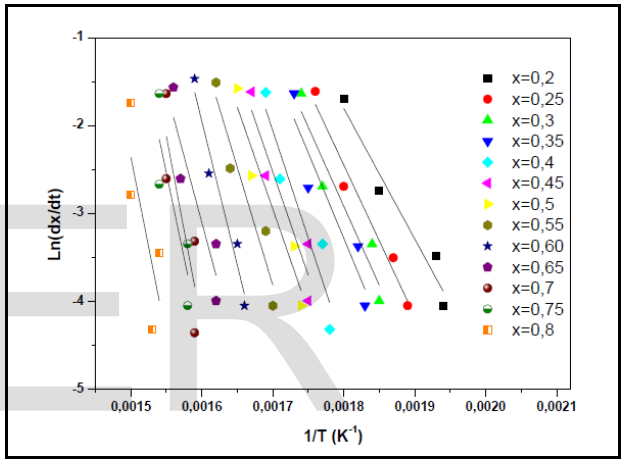

Fig. 14. Friedman plots for cellulose of COMWW thermal degradation

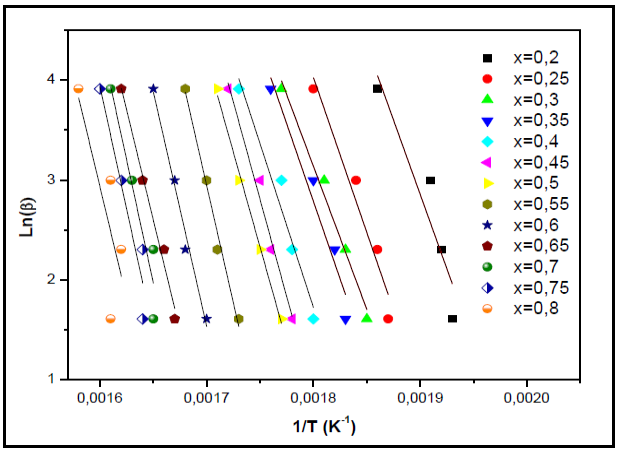

Fig. 12. Ozawa-Flynn-Wall plots for cellulose of OMSW thermal degradation

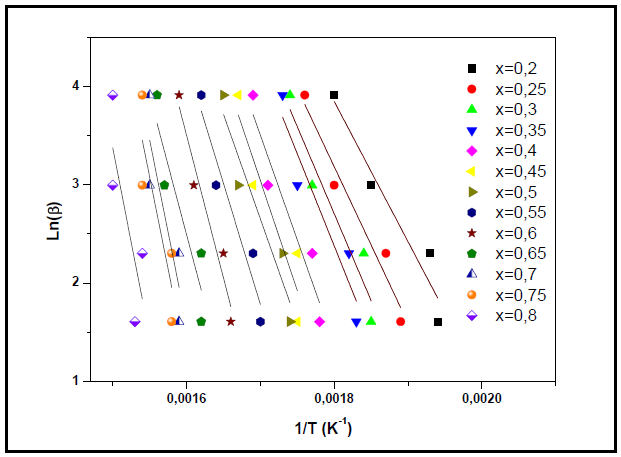

Fig. 15. Ozawa-Flynn-Wall plots for hemicellulose of COMWW thermal degradation

3.3 Determination of the degradation mechanism using Coats-Redfern and Criado methods

A model or kinetic method is a mathematical, theoretical description of what occurs experimentally. In solid state reactions, a model can illustrate a particular reaction type and interpret that mathematically into a rate equation. Many methods and models have been proposed in solid-state kinetics, and these methods have been developed based on certain mechanistic assumptions. Other methods are more empirically based, and their mathematics facilities data analysis with little mechanistic meaning. Therefore, different rate expressions are produced from these models.

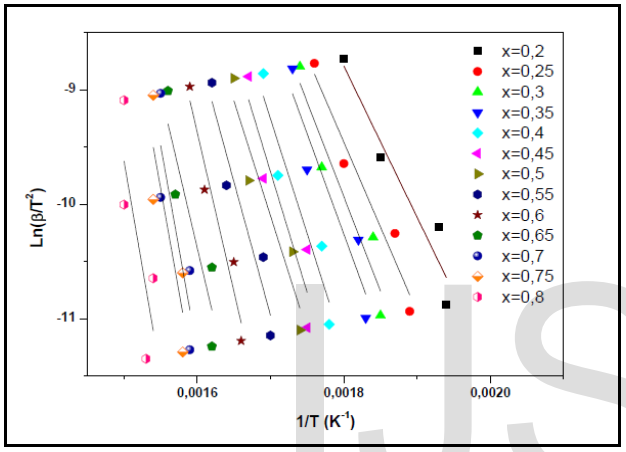

Fig. 16. Vyazovkin plots for cellulose of COMWW thermal degradation

TABLE 7
ACTIVATION ENERGIES OF HEMICELLULOSE OF OMSW OBTAINED BY COATS-REDFERN METHOD

Model	Activation Energy (KJ/mol)	Coefficient R^2
D1	180	0.9519
D2	182	0.9602
D3	201	0.9354
D4	194	0.9615
P2	73	0.8612
P3	90	0.6467
P4	47	0.7001
R2	147	0.9523
R3	149	0.9566
F1	**160**	**0.9630**
F2	187	0.9385
F3	191	0.8872
A2	128	0.9304
A3	148	0.8495
A4	91	0.5857

TABLE 8
ACTIVATION ENERGIES OF CELLULOSE OF OMSW OBTAINED BY COATS-REDFERN METHOD

Model	Activation energy (KJ/mol)	Coefficient R^2
D1	200	0.8600
D2	193	0.8899
D3	203	0.9266
D4	190	0.9031
P2	31	0.7686
P3	15	0.6630
P4	11	0.4989
R2	177	0.8966
R3	180	0.9159
F1	205	0.9488
F2	**218**	**0.9786**
F3	240	0.9623
A2	161	0.9333
A3	153	0.9105
A4	149	0.8755

TABLE 9
ACTIVATION ENERGIES OF HEMICELLULOSE OF COMWW OBTAINED BY COATS-REDFERN METHOD

Modèle	Energie d'activation (KJ/mol)	Coefficient de corrélation
D1	**140**	**0.9870**
D2	149	0.9724
D3	152	0.9785
D4	147	0.9749
P2	21	0.8965
P3	17	0.7248
P4	13	0.1679
R2	117	0.9678
R3	128	0.9716
F1	129	0.9755
F2	131	0.9506
F3	130	0.8996
A2	120	0.9556
A3	118	0.9039
A4	109	0.7194

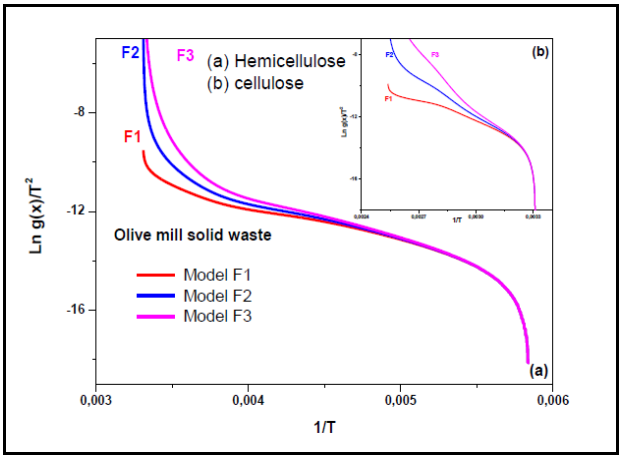

Fig. 17. Plots of $\ln(g(x)/T^2)$ versus 1/T for F_n model for OMSW, (a) cellulose (b) hemicellulose

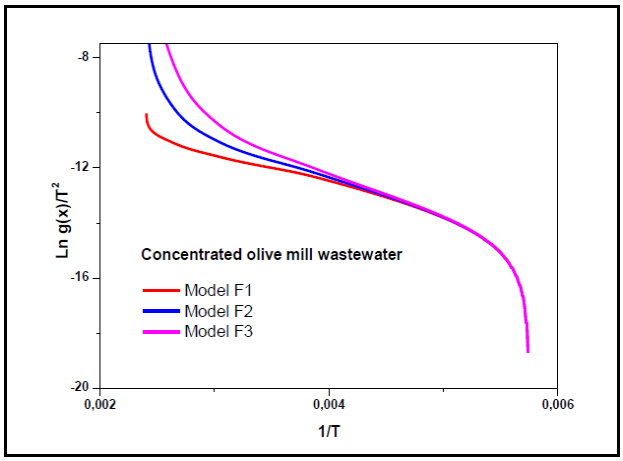

Fig. 18. Plots of $\ln(g(x)/T^2)$ versus 1/T for F_n model for cellulose of COMWW

TABLE 10
ACTIVATION ENERGIES OF CELLULOSE OF COMWW OBTAINED BY COATS-REDFERN METHOD

Modéle	La pente	Coefficient de corrélation
D1	*167*	*0.8749*
D2	*172*	*0.9041*
D3	*177*	*0.9359*
D4	*173*	*0.9159*
P2	*23*	*0.6725*
P3	*20*	*0.3266*
P4	*8*	*0.1874*
R2	*251*	*0.8982*
R3	*253*	*0.9172*
F1	*235*	*0.9463*
F2	***270***	***0.9537***
F3	*281*	*0.9206*
A2	*134*	*0.9094*
A3	*129*	*0.8274*
A4	*115*	*0.6197*

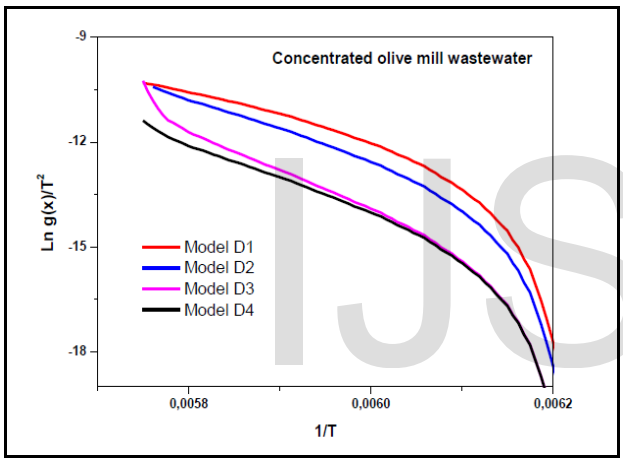

Fig. 19. Plots of $\ln(g(x)/T^2)$ versus 1/T for D_n model for hemicellulose of COMWW

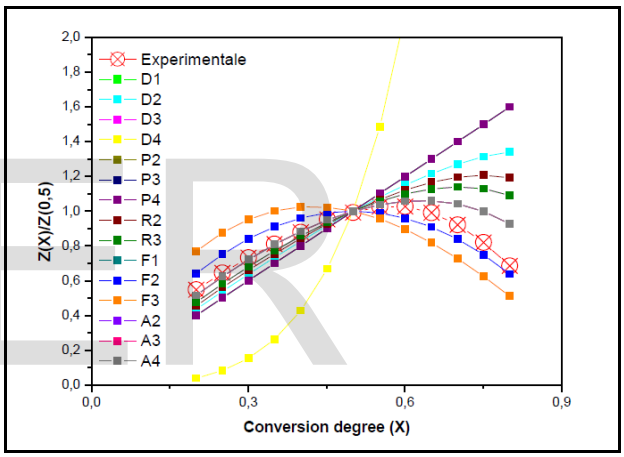

Fig. 21. Masterplots of different kinetic models and experimental data 10 °C/min for cellulose of OMSW

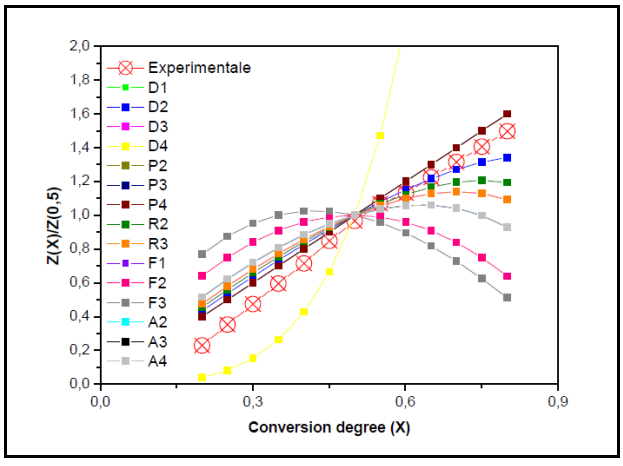

Fig. 20. Masterplots of different kinetic models and experimental data 10 °C/min for hemicelluloses of OMSW

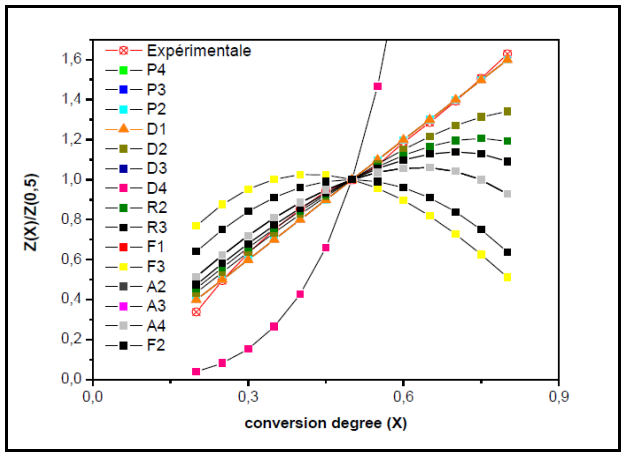

Fig. 22. Masterplots of different kinetic models and experimental data 10 °C/min for hemicellulose of COMWW

In order to find the kinetic model of thermal degradation of olive mill solid waste (OMSW) and olive mill wastewater (OMWW), the Coats-Redfern and Criado methods were chosen as they involve the degradation mechanisms. To determine the most probable model, Coats-Redfern method was used, According to Eq (10), activation energy for every $g(x)$ function listed in table 3 can be calculated at 10 °C/min (figs 3 and 4), from fitting $ln(g(x)/T^2)$ versus $1/T$ plots. The activation energies and coefficient correlations at 10 °C/min are tabulated in tables 7-10, for olive mill solid waste and olive mill wastewater (including both compounds cellulose and hemicelluloses). To obtain the degradation mechanism of olive mill solid waste, we have compared the activation energies obtained by the models above, according to table 7 and 8, it could be found that the E values of cellulose and hemicellulose of olive mill solid waste corresponding to mechanisms F_1 (160 KJ/mol) and F_2 (218 KJ/mol) are in agreement with the values obtained by Friedman, Flynn-wall-ozawa, Vyazovkin and Kissinger methods (FR=176 KJ/mol, OFW=167 KJ/mol, VYA=150 KJ/mol and KAS= 161 KJ/mol for hemicellulose and FR=235 KJ/mol, OFW=210 KJ/mol, VYA=212 KJ/mol and KAS= 222 KJ/mol for cellulose). Otherwise, the mechanisms of thermal degradation of olive mill wastewater agrees with mechanim D_1 (140 KJ/mol) for hemicellulose and F_2 (270 KJ/mol) for cellulose of OMWW. These results are in agreement with activation energies obtained by Kissinger, OFW, Friedman and Vyazovkin methods (FR=145 KJ/mol, OFW=137 KJ/mol, VYA=132 KJ/mol and KAS= 154 KJ/mol for hemicellulose and FR=275 KJ/mol, OFW=255 KJ/mol, VYA=255 KJ/mol and KAS= 237 KJ/mol for cellulose).

Fig 17, 18 and 19 shows the plot of $ln\ (g(x)/T^2)$ versus $1/T$ for different models. All models have a similar trend with correlation coefficient greater than 0.90 (> 0.9). According to Coats-Redfern equation, if a correct model is selected for the reaction, the plot of $ln\ (g(x)/T^2)$ versus $1/T$ will be linear as possible with high-correlation coefficient. One can say that the Coats-Redfern method reliability is not enough and cannot be used to kinetics assessment of reactions. From this point of view the use of the method of Criado is very important, this method gives us more information and can be additional to Coats-Redfern method. The used models and the expressions of associated functions $f(x)$ and $g(x)$ are shown in table 3. The master curve plots $Z(X)/Z(0.5)$ versus x for different mechanisms according to the Criado method Eq(11) for olive mill wastewater and olive mill solid waste degradation is illustrated ins Figs 20-23. As can be seen, the comparison of the experimental master plots with theoretical, ones revealed that the kinetic process for the degradation of cellulose of olive mill solid waste and olive mill wastewater was most probably described by the reaction order F_2 (F_n model), while the degradation of hemicellulose of olive mill wastewater corresponding to D_1 Diffusion (D_n model) and the degradation of hemicelluloses of olive mill solid waste was F_1 (reaction order F_n).

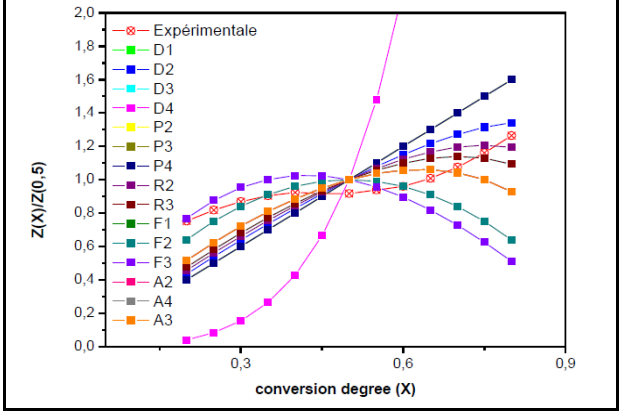

Fig. 23. Masterplots of different kinetic models and experimental data 10 °C/min for cellulose of COMWW

One of the major differences between homogenous and heterogeneous kinetics is the mobility. Diffusion (Model D_n) is characterized by the mobility of constituents in the system. While reactant molecules are usually readily available to one another, solid-state reactions often occur between crystal lattices or with molecules that must permeate into lattices where motion is restricted and may depend on lattice defects. A product layer may increase where the reaction rate is controlled by the movement of the reactants to or products from the reaction interface. Solid-state reactions are not usually controlled by mass transfer except for few reversible reactions or when large evolution or consumption of heat occurs. Diffusion (D_n) usually plays a role in the rates of reaction between two reaction solids, when reactants are in separate crystal lattices. In diffusion-controlled reactions, the rate of product formation decreases proportionally with the thickness of the product barrier layer. Concerning reaction order, order-based models (F_n) are the simplest models as they are similar to those used in homogeneous kinetics. In these models, the reaction rate is proportional to concentration, amount or fraction remaining of reactant raised to a particular power which is the reaction order.

4 Conclusion

The kinetics of thermal degradation of olive mill solid waste (OMSW) and Concentrated olive mill wastewater (COMWW) was accuretly determined from a series of experiments at four heating rates (5, 10, 20 and 50 °C/min. the activation energy was calculated by the isoconversional methods without previous assumption regarding the conversion model fulfilled by the reaction. The activation energy was found practically constant in the range 0.2-0.8 conversion range for both hemicellulose and cellulose of OMSW and COMWW, this suggesting that the pyrolysis was a two-step process with an activation

energy of 150-176 KJ/mol for hemicelluloses and 212-235 KJ/mol for cellulose of OMSW and 132-154 KJ/mol for hemicelluloses and 237-283 KJ/mol for cellulose of COMWW. Finally, Coats-Redfern and Criado methods were successfully utilized to predict the reaction mechanism of thermal degradation of OMSW and COMWW. The pyrolysis reaction models of OMSW and COMWW are described by reaction order F_n, second-order (F_2) for cellulose and hemicellulose of OMSW and COMWW. Whereas the hemicellulose of OMSW and COMWW following a kinetic model of F_1 (First order) and D_1 (One-dimensional diffusion), respectively.

References

[1] A.G.D. Santos, V.P.S. Caldeira, M.F. Farias, A.S. Araújo, L.D. Souza, A.K. Barros,Characterization and kinetic study of sunflower oil and biodiesel, *Journal ofThermal Analysis and Calorimetry* 106 (2011) 747–751.

[2] Vecchio, L. Cerretani, A. Bendini, E. Chiavaro, Thermal decompositionstudy of monovarietal extra virgin olive oil by simultaneous thermogravime-try/differential scanning calorimetry: relation with chemical composition,*Journal of Agricultural and Food Chemistry* 57 (11) (2009) 4793–4800.

[3] K.D. Maher, D.C. Bressler, Pyrolysis of triglyceride materials for the produc-tion of renewable fuels and chemicals, *Bioresource Technology* 98 (2007)2351–2368.

[4] F. Kotti, E. Chiavaro, L. Cerretani, C. Barnaba, M. Gargouri, A. Bendini, Chemicaland thermal characterization of Tunisian extra virgin olive oil from Chetoui andChemlali cultivars and different geographical origin, *European Food Researchand Technology* 228 (5) (2009) 735–742.

[5] Tukker A. Plastic waste feedstock recycling, chemical recycling and incineration, *Rapra Review Reports*, vol. 3 (4), Report 148, Shropshire, UK: *Rapra Technology* Ltd, 2002.

[6] Marin N, Collura S, Sharypov V I, Beregovtsova N G, Baryshnikov S V, Kuznetsov B N. Co-pyrolysis of wood biomass and synthetic polymer mixtures: Part II Characterization of liquid phases. *J Anal Appl Pyrolysis*, 2002, 65(2): 41–55.

[7] Shafizadeh F, Mcginnis G D. Chemical composition and thermal analysis of cottonwood. *Carbohydr Res*, 1971, 16(2): 273–277.

[8] Kastanaki E, Vamvuka D. A comparative reactivity and kinetic study on the combustion of coal-biomass char blends. *Fuel* 2006; 85:1186–93.

[9] Kazagic A, Smajevic I. Synergy effects of co-firing wooden biomass with Bosnian coal. *Energy* 2009; 34:699–707.

[10] Kumar A, Wang L, Dzenis YA, Jones DD, HannaMA. Thermogravimetric characterization of corn Stover as gasification andpyrolysis feedstock. *Biomass and Bioenergy* 2008; 32:460–7.

[11] Lester E, Gong M, Thompson A. A method for apportionment in biomass/coal using thermogravimetric analysis. *Journal of Analytical and Applied Pyrolysis* 2007; 80:111–7.

[12] Lopez MC, Blanco CG, Martimez-Alonso A, Tascou JMD. Composition of gases released during olive stones pyrolysis. *Journal of Analytical and Applied Pyrolysis* 2002; 65:313–22.

[13] Masghouni M, Elhassayri M. Energy applications of olive-oil industry by-products—I. The exhaust foot cake. *Biomass and Bioenergy* 2000; 18:257–62.

[14] Milosavljevic I, Suuberg EM. Cellulose thermal decomposition kinetics: global mass loss kinetics. *Industrial and Engineering Chemistry Research* 1995; 34:1081–91.

[15] Muller-Hagerdorn M, Bockhorn H, Krebs L, Muller U. Investigation of thermal degradation of three wood species as initial steps in combustion of Biomass. *Proceedings of the Combustion Institute* 2002; 29:399–406.

[16] Caputo Antonio C, Scacchia F, Pelagagge PM. Disposal of by-products in olive oil industry: waste-to-energy solutions. *Applied Thermal Engineering* 2003; 23:197–214.

[17] Della Rocca PA, Horowitz GI, Bonelli P, Cassanello MC, Cukierman AL. Olive stones pyrolysis: chemical, *textural and kinetics characterization.* In: Bridgwater AV, Boocock DGB, editors. Developments in thermo-chemical biomass conversion. *London: Blackie*; 1997. p. 176–89.

[18] Demirbas A. Effects of temperature and particle size on bio-char yield from pyrolysis of agricultural residues. *Journal of Analytical and Applied Pyrolysis* 2004; 72:243–8.

[19] Dornburg V, Faaij PC, Meuleman B. Optimising waste treatment systems, Part A: Methodology and technological data for optimizing energy production and economic performance. *Resources, Conservation and Recycling* 2006; 49:68–88.

[20] Gani A, Naruse I. Effect of cellulose and lignin content on pyrolysis and combustion characteristics for several types of biomass. *Renewable Energy* 2007; 32:649–61.

[21] Garcia-Iba ˜nez P, Sanchez M, Cabanillas A. Thermogravimetric analysis of olive-oil residue in air atmosphere. *Fuel Processing Technology* 2005; 87:103–7.

[22] T.R. Ingraham, P. Marrier, Can. *J. Chem. Eng*. 42 (1964) 161.

[23] H.E. Kissinger, *J. Res. Nat. Bur. Stand*. 57 (1956) 217–221.

[24] Kissinger HE. Reaction kinetics in differential thermal analysis. *Anal Chem* 1957; 29:1702–6.

[25] Akahira T, Sunose T. Trans joint convention of Four Electrical Institutes, paper no. 246, 1969 research report. *Chiba Institute of Technology Sci Technol*, vol.16; 1971. p. 22–31.

[26] Coats AW, Redfern J. Kinetic parameters from thermogravimetric data. *Nature* 1964; 201:68–9.

[27] Flynn J, Wall LA. Quick direct method for the determination of activation energy from thermogravimetric data. Polym Lett 1966; 4: 323–8.

[28] Criado JM. Kinetic analysis of DTG data from master curves. *Termochim Acta* 1978; 24:186–9.

[29] M. Y. Guida, H. Bouaik, A. Tabal, K. EL harfi, A. Solhy, A. Barakat, A. Aboulkas, A. Hannioui, Thermochemical treatment of olive mill solid waste and olive mill wastewater: pyrolysis Kinetics, *2015 J Therm Anal Calorim*, 123 (2) : pp 1657-1666.

[30] A. Ammar Khawam, and Douglas R. Flanagan, Solid-State Kinetic Models: Basics and Mathematical Fundamentals, *J. Phys. Chem. B*, 2006, 110 (35), 17315-17328.